AD-A280 851

COPY 1

paper no. 55-SA-78 0

The American Society of Mechanical Engineers

29 WEST 39TH STREET, NEW YORK 18, NEW YORK

RESISTANCE COEFFICIENTS FOR ACCELERATED AND DECELERATED FLOWS
THROUGH SMOOTH TUBES AND ORIFICES

J. W. Daily, Mem. ASME
Associate Professor of Hydraulics
Massachusetts Institute of Technology
Cambridge, Massachusetts

W. L. Hankey, Jr., 1st Lieut. USAF
Project Engineer, Transonic Wind Tunnel
Wright Patterson Air Force Base
Ohio

R. W. Olive, Mem. ASME
Manufacturing Supervision Trainee
Manufacturing Training Program
General Electric Company - River Works
Lynn, Massachusetts

and

J. M. Jordaan, Jr.
Research Assistant, Hydrodynamics Laboratory
Massachusetts Institute of Technology
Cambridge, Massachusetts

DTIC
ELECTE
JUN 09 1994
S
G
D

LIBRARY COPY

ADVANCE COPY: Released for general publication upon presentation.

Printed in U.S.A.

Price: 50 cents per copy
(25 cents to ASME members)

94 6 8 041

DISCLAIMER NOTICE
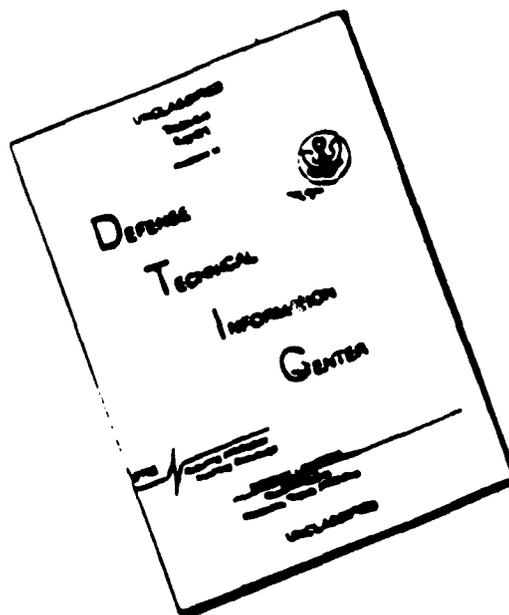
Resistance Coefficients for Accelerated and Decelerated Flows Through Smooth Tubes and Orifices

by

J. W. Daily, W. L. Hankey, Jr., R. W. Olive and J. M. Jordaan

INTRODUCTION

In the prediction of transients involving hydrodynamic or aerodynamic phenomena, it has been customary to calculate pressure variation and fluid resistance neglecting possible effects of unsteadiness on the mechanics of the fluid motion. There are several areas for which knowledge of the effects of unsteadiness would be useful. Included, for example, are transient resistance and stability of accelerating missiles and other immersed objects, flow meter coefficients with pulsating flows, and transient hydrodynamic performance of pumps, compressors and turbines. The latter is a case where under many circumstances steady state performance has been used with good results in predicting transient pressures and machine accelerations and decelerations. Yet, recently, in connection with pumps of special design, discrepancies between measured and calculated transients have indicated what is probably an effect of unsteadiness on the basic fluid motion. In all cases a basic question is the effect of unsteadiness on fluid shear and turbulence generation, and the resulting effects on the inertial and frictional components contributing to the instantaneous total potential drop.

This paper summarizes the results of investigations in the M. I. T. Unsteady Flow Water Tunnel (Ref. 1, 2, 3, 4) of accelerated and decelerated flow through uniform conduits and orifices in conduits. In the uniform conduit shear and turbulence is generated through boundary layer friction and is essentially uniform along the duct. The orifices cause separation and jet formation with accompanying high shear and turbulence which varies along the duct as the jet diffuses and the turbulence is dissipated.

UNSTEADY FLOW EQUATIONS

As a basis for analyzing experimental results, the following momentum analysis was made in which the effects of all the variables including turbulence are considered. Thus while the equations are reduced ultimately to essentially a one-dimensional form, more insight is given to the significance of each term than is readily apparent from an ordinary one-dimensional analysis.

Consider a constant diameter conduit which may be unobstructed or may contain constrictions such as orifices or venturi sections. Let the dotted boundary shown in Figure 1 define a control volume for a general case.
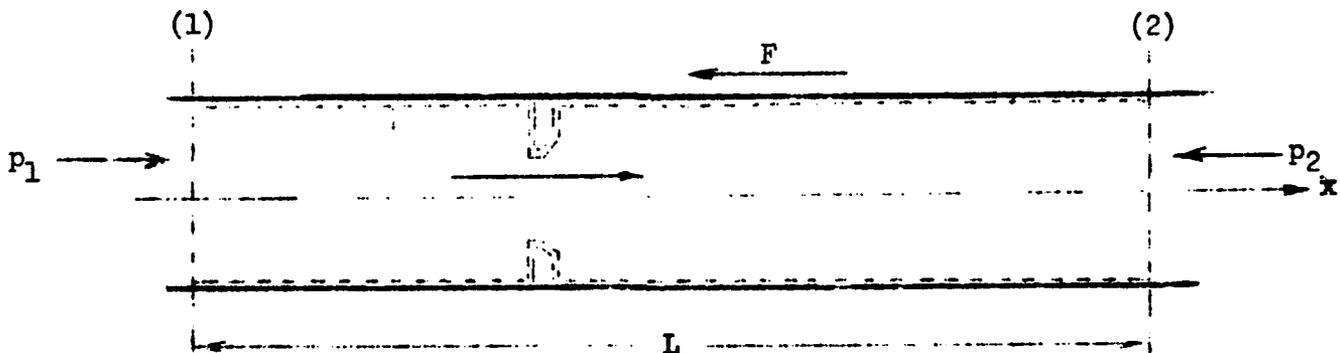
Figure 1

Applying the momentum principle to unsteady turbulent liquid flow through such a system, we can write the instantaneous balance

(External Forces) $= \sum$ (Net flux of momentum from control volume + rate of change of momentum within the volume)

or, for the x-direction

$$\int^{A_1} P_1 dA - \int^{A_2} P_2 dA - F = \int^{A_2} \rho U_2^2 dA - \int^{A_1} \rho U_1^2 dA + \int^{\Psi} \rho \frac{\partial U}{\partial t} d\Psi \qquad (1)$$

where P = x-component of local pressure intensity

F = lumped boundary resistance due to wall shear and any constrictions

U = local velocity

Ψ = liquid volume within control surface

Analogous to "steady" turbulent flow we will assume that at each instant during a transient the velocity field can be described as a "mean flow" plus a "fluctuating flow" and introduce the usual notation

$$U = u + u' \qquad (2)$$

Here then u is a kind of mean value like the temporal mean value of statistically steady turbulent motion. Using Eq. (2) gives

$$\int^{A_1} P_1 dA - \int^{A_2} P_2 dA - F = \int^{A_2} \rho u_2^2 dA - \int^{A_1} \rho u_1^2 dA + \int^{A_2} \rho u_2'^2 dA - \int^{A_1} \rho u_1'^2 dA$$

$$+ 2\int^{A_2} \rho u_2 u_2' dA - 2\int^{A_1} \rho u_1 u_1' dA + \int^{\Psi} \rho \frac{\partial u}{\partial t} d\Psi + \int^{\Psi} \rho \frac{\partial u'}{\partial t} d\Psi \qquad (3)$$

At this stage it is customary in analyzing turbulent flows to take temporal mean values of all terms in the equations in order to obtain a relation governing the main flow. This ignores the contribution of the terms that are linear in the turbulent components, because they drop out in the averaging process. For very rapid changes of the main flow this may not be justified. We will leave the equation in terms of the instantaneous velocity fluctuations so that the relative importance of the instantaneous turbulence can be evaluated. Using the definitions:

$$p = \frac{\int P dA}{A} = \text{average pressure intensity over the cross section}$$

$$U_o = \frac{Q}{A} = \text{instantaneous cross-sectional mean velocity in conduit}$$

$$K_a = \frac{P_1 - P_2}{\rho \frac{U_o^2}{2}} = \text{unsteady flow coefficient of total drop in potential} \qquad (4)$$

$$K = \frac{F}{\rho \frac{U_o^2 A}{2}} = \text{unsteady flow coefficient of boundary resistance} \qquad (5)$$

$$\alpha = \frac{\int^A \frac{u^2}{2} dA}{U_o^2 A} = \text{distribution factor for mean velocity} \qquad (6)$$

$$I = \frac{\int^A u'^2 dA}{U_o^2 A} + \frac{2\int^A u\, u' dA}{U_o^2 A} = \text{distribution factor for turbulent fluctuations} \qquad (7)$$

and the approximation that $\frac{u}{U_o}$ is independent of time, Eq. (3) is expressed dimensionlessly as

$$K_a = K + 2\left\{(\alpha_2 - \alpha_1) + (I_2 - I_1)\right\} + 2\frac{\partial U_o}{\partial t} \frac{\int^{\Psi} \frac{u}{U_o} d\Psi + \int^{\Psi} \frac{u'}{U_o} d\Psi}{U_o^2 A}$$

$$= K + 2\left\{(\alpha_2 - \alpha_1) + (I_2 - I_1)\right\} + c_1 \frac{2a \Psi}{U_o^2 A} \qquad (8)$$

where

$$\frac{\partial U_o}{\partial t} = a = \text{acceleration of the mean flow in the conduit} \qquad (9)$$

$$c_1 = \frac{\int^{\Psi} \frac{u}{U_o} d\Psi + \int^{\Psi} \frac{u'}{U_o} d\Psi}{\int^{\Psi} d\Psi} = \text{inertial coefficient} \qquad (10)$$

The last term in Eq. (8) is the dimensionless force of inertia of the turbulent fluid to local accelerations. The second right-hand term gives the effect of non-uniformity of the mean flow and turbulence intensity between sections 1 and 2. It is the dimensionless x - component of the flux of momentum of the absolute motion. While the effect of turbulence appears explicitly only in the second and third right-hand terms, it also appears indirectly in the resistance coefficient K. The velocity and turbulence distributions within the liquid volume are interdependent with the boundary shears and pressures and hence the boundary resistance.

Also to the extent that the establishment of each instantaneous velocity and turbulence distribution requires some absolute time interval for the adjustment from a previous condition, the relative magnitudes of the several terms in this force-momentum balance may depend on the rate of change of acceleration as well as the magnitude of the acceleration.

While Eq. (8) is useful for qualitative indication of how turbulence, flow uniformity and acceleration affect the total potential drop and boundary resistance, it cannot be used for quantitative comparisons because the required instantaneous velocity and turbulence distributions cannot be calculated or measured. Because of this and because it is desirable to make comparisons with steady-state conditions corresponding to given instantaneous rate of discharge we introduce the following simplifications:

Let:

$$K_u = K + 2\left\{(\alpha_2 - \alpha_1) + (I_2 - I_1)\right\}$$
$$= K_s + K_t \tag{11}$$

where

K_u = unsteady flow coefficient of boundary resistance and momentum flux of absolute local velocity

K_s = one-dimensional steady state "resistance" coefficient

K_t = correcting coefficient to measure the additional transient effects on boundary resistance and momentum flux of absolute local velocity

Eq. (8) becomes

$$K_a = K_s + K_t + c_1 \frac{2a \Psi}{U_o^2 A} \tag{12}$$

For steady flow this reduces to the relation given by the conventional one-dimensional energy equation where the resistance coefficient is taken as a measure of the energy dissipation.

Eq. (12) can be simplified further with the aid of an analogy to Schonfeld's analysis for smooth round tubes (Ref. 5). Schonfeld presents the following solution for the special case of slowly varied motion in which the resistance dominates (as opposed to quickly varied motion where the inertia dominates).

$$P_1 - P_2 = \frac{\rho\, g L}{R_h C'^2}\, \frac{Q^2}{A^2} + N\frac{dQ}{dt} \tag{13}$$

where

Q = rate of discharge
R_h = hydraulic radius
C' = steady flow Chezy coefficient"
$$N = \frac{\rho\, L}{A}\left[1.0 + \frac{234}{(C' + 14.0)^2}\right] \tag{14}$$

By substituting $C' = \sqrt{\frac{8g}{f_s}}$ (f_s = steady flow friction factor),

$R_h = \frac{D}{4}$ and $Q = AU_o$, Eq. (14) can be rewritten for the tunnel test section thus

$$\frac{P_1 - P_2}{\rho\, \frac{U_o^2}{2}} = \frac{2a L}{U_o^2} + f_s \frac{L}{D} + \frac{0.91}{(\frac{1}{\sqrt{f_s}} + 0.87)^2}\, \frac{2a L}{U_o^2} \tag{15}$$

We note that this can be put in the form of Eq. (2) if we make the substitutions

$$\frac{2aL}{U_o^2} = \frac{2a \Psi}{U_o^2 A}$$

$$c_1 = 1.00$$

$$K_s = \frac{f_s L}{D} \tag{16}$$

$$K_t = \frac{0.91}{(\frac{1}{\sqrt{f_s}} + 0.87)^2} \frac{2aL}{U_o^2} \tag{17}$$

As these substitutions indicate, Schonfeld's analysis considers the turbulence to be fully developed at every instant and uniform conditions to exist along the length of the conduit. Thus the value $c_1 = 1.00$ implies that the mean value of the turbulent fluctuations over the liquid volume of the uniform tube is zero at all times so that the inertial coefficient is merely

$$c_1 \approx \frac{\int^\Psi \frac{u}{U_o} d\Psi}{\int^\Psi d\Psi} = 1$$

Furthermore, if similar flow conditions exist at all sections along the conduit, the term $(\alpha_2 - \alpha_1)$ will be zero and the term $(I_2 - I_1)$ will approach zero for sufficiently random values of u' at each instant over each annular increment of flow area at the two sections. Thus K_t as given by Eq. (17) implies no influence of non-uniformity in velocity or turbulence.

Returning now to the more general case which may include tubes with constrictions, let us write in analogy to Eq. (17)

$$K_t = c_2 \frac{2a \Psi}{U_o^2 A} \tag{18}$$

In Eq. (18) c_2 is a measure of the deviations, due to unsteadiness of the boundary resistance and flux of momentum. Using Eq. (18), Eq. (12) reduces to:

$$K_a \cong K_s + c \frac{2a \Psi}{U_o^2 A} \tag{19}$$

with
$$c = c_1 + c_2$$

We can also write this as

$$\frac{K_a}{K_s} = 1 + c \frac{2a\Psi}{K_s U_o^2 A} \tag{20}$$

or, noting from Eqs. (11) and (12) that

$$K_u = K_s + K_t = K_a - c_1 \frac{2a \Psi}{U_o^2 A}$$

$$\frac{K_u}{K_s} = 1 + c_2 \frac{2a \Psi}{K_s U_o^2 A} \tag{21}$$

Equations (19), (20) and (21) are exact statements of the balance of forces specified by the momentum principle. Moreover, to the extent that the quantity $2\{(\alpha_2 - \alpha_1) + (I_2 - I_1)\}$ in Eq. (11) approaches zero, K_u becomes equal to K and the equations will be useful for comparing the steady and unsteady boundary resistance at given instantaneous discharge rates. Here we note, that as for a clear conduit, flow through a constricted conduit having a test length L much longer than the disturbed flow zone caused by the constriction, should exhibit approximately the same velocity and turbulence distributions at sections 1 and 2. Hence, only a small error is introduced by assuming $K_u = K$. In this case, it will be noted from Eq. (21) that for accelerated flow where a is positive, positive values of c_2 will indicate that _more_ boundary resistance is developed than for steady flow and vice versa. For decelerated flow where a is negative, positive c_2 will indicate that _less_ boundary resistance is developed than for steady flow and vice versa.

Note that in c_1, as defined by Eq. (10), the magnitude of the first term will be unity or larger unless there are flow reversals giving negative u values. Again as for the clear conduit, the mean value of the turbulent fluctuations over the liquid volume of the constricted conduit is expected to be very small if not zero, making the second term of c_1 negligible. Let us introduce then the approximation for c_1

$$c_1 \approx \frac{1}{L} \int_0^L \frac{V}{U_0} \, dx \qquad (22)$$

where V = average velocity over the cross section of the main stream (jet) at any x.

This definition permits evaluation of c_1 from a flow net of the jet profile through the constriction. By this definition also c_1 will tend toward a constant value if the dimensionless velocity along the main stream (or jet) remains independent of the unsteadiness. An experimental determination of the coefficient c and a calculated value of c_1 will permit evaluation of c_2 and K_u. With these simplifications, the resulting c_2 will absorb the difference between the true inertial coefficient and the value calculated by Eq. (22), as well as the durations, due to unsteadiness, of the boundary resistance and flux of momentum.

The parametric form of Eqs. (20) and (21) makes it convenient to evaluate the comparison between steady and unsteady behavior from a simple series of measurements of total potential drop along the conduit versus instantaneous flow rate. From each such basic experiment, the comparison can be obtained for each of a range of values of the ratio $\frac{a\Psi}{U_0^2 A} = \frac{aL}{U_0^2}$.

Finally note that the term $\frac{a\Psi}{U_0^2 A} = \frac{aL}{U_0^2}$ is a parameter proportional to the ratio of local to convective acceleration. If all the effects of unsteadiness are fundamentally dependent on the acceleration, the coefficients in Eqs. (20 and (21) will be constants, otherwise not.

EXPERIMENTAL APPARATUS

The apparatus used for these experiments is a non-return unsteady flow water tunnel (Ref. 6). As shown by the schematic section in Figure 2, the tunnel consists of two cylindrical tanks mounted one above the other and connected by a 1-inch diameter smooth brass conduit 99 diameters in length. This conduit constitutes the test section in which constrictions such as orifices or venturi sections can be placed. Water is caused to flow from one tank to the other under pneumatic control. Compressed air is admitted to the spaces above the water surfaces in the two tanks to provide a driving force for a desired flow rate and acceleration or deceleration. To obtain the desired ranges of acceleration and pressure in the working section, compressed air must be admitted to or released from either tank according to some time schedule. To prevent cavitation and the introduction of air into the piezometric system, the test section is maintained at positive pressure by throttling the exhaust from the bottom tank. The square edged orifices employed were dimensioned according to ASME standards and constructed from 0.102" thick sheet brass. The conduit and orifice combinations used and the principal dimensional data and location of piezometer taps are given in Table I and Figure 3.

Table I

Test Combinations and Principal Dimensions

	Area ratio	$\dfrac{d}{D}$	$\dfrac{d_j}{D}$	Assumed jet dimensions — Diffusion angle for 4 dia. expansion
Smooth Tube	1.0	1.0	.	
Orifice in Tube	0.7	0.837	0.72	$4°22'$
Orifice in Tube	0.5	0.707	0.59	$6°38'$
Orifice in Tube	0.3	0.548	0.44	$9°06'$
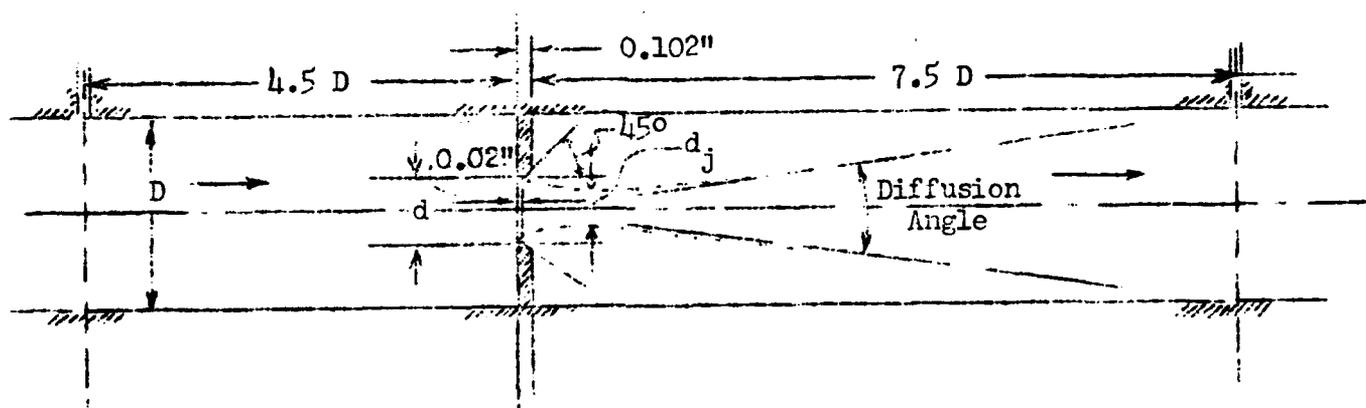
Figure 3

In all experiments the beginning of the test length over which potential drops were measured was located well beyond the calculated transition distance

necessary to establish a fully developed turbulent velocity profile in the 1-inch tube. In most tests the test length began at approximately 33 diameters from the entrance nozzle, the orifice being located at "x" = 37.5 diameters. (See Figure 2) In some cases a 28 diameter approach was used ("x" = 32.5 diameters). The actual test length L was 27 diameters for the unobstructed tube and 12 diameters for the cases of orifice constricted tube. For the latter, the piezometer taps were located 4.5 diameters upstream and 7.5 diameters downstream of the orifice plate. The 7.5 diameter downstream distance was chosen to include the expected zone of influence of the orifice on the local flow conditions (Ref. 7). Some measurements were made also with the downstream piezometer taps 22.5 diameters from the orifice as checks in case the orifice disturbance persisted for greater distances for unsteady flow than for steady. The results of these checks did not alter the conclusions drawn from the measurements over the shorter distance.

The nozzle at the inlet to the working section is used for flow measurements. The instantaneous pressure drops recorded during unsteady flows are corrected to account for the inertia force due to the local acceleration of the fluid through the nozzle. The correction calculated assuming potential flow 0.2 dU_o/dt.

The several differential pressures were measured with diaphragm type pressure cells in which the diaphragm deflection actuates a differential transformer. Each pressure gage signal is sent through a separate amplifying and detecting unit and is then recorded versus time. Two amplifying-recording systems were used during the experiments; in one, a photographic record was obtained using a Hathaway Type S8-C oscillograph; in the other, the record was traced with a temperature-stylus on Sanborn "Permapaper" using a four-channel Sanborn Recorder, Model 150. Measured natural frequencies of the pressure cells and oscillograph recording system connected as for testing including water-filled lead lines, exceeded 165 cycles per second. With the Sanborn recorder the limit of accurate response is about 100 cycles per second. Instantaneous differential pressures were evaluated using static calibrations of each gage before and after test runs.

EXPERIMENTAL PROGRAM

The range of variables for the experiments reported here are given in Table II. As the table indicates, a range of velocities and accelerations or decelerations were included. In addition, the several tests included different rates of change of acceleration.

Acceleration tests were made from zero velocity or were preceded by an initial period of steady flow. All deceleration tests were preceded by an initial period of steady flow. At the start of each unsteady period was an initial impulse phase during which the acceleration (or deceleration) changed rapidly ($|\frac{da}{dt}| \gg 0$).

Following this was an "established" phase, distinguished by either constant or more slowly changing acceleration. In general, the acceleration or deceleration varied continuously although in the case of the uniform diameter conduit, several runs, each with essentially constant deceleration, were obtained. The period of the initial impulse phase varied and it was not always possible to obtain reliable recordings of the instantaneous pressures. Typical test results appear in Figures 8a and 8b. These diagrams show instantaneous conduit velocity U_o, acceleration dU_o/dt and total potential head drop H_a as calculated from oscillograph recordings.

Table II

Range of Experimental Investigation

Equivalent area ratio	Maximum conduit velocity at steady state discharge fps	Maximum conduit Reynolds Number	Maximum throat Reynolds Number	Conduit acceleration range fps^2 max. ave.		Conduit deceleration range fps^2 max. ave.	
Orifices:							
0.7	38.7	320,000	580,000	80	40	50	25
0.5	29.75	248,000	720,000	60	30	50	25
0.3	18.00	150,000	770,000	30	15	30	15
Smooth Conduit:							
1.0	9 to 60*	500,000	---	80	40		
	36 to 18**	300,000	---			7, 11, 16, 20	

* Runs 39, 40, by Deemer for accelerated flow.
** Runs UJ, by Jordaan for decelerated flow.

From such data values of $K_a = \dfrac{H_a}{U_o^2/2g}$ versus $\dfrac{aL}{U_o^2}$ were obtained for successive time intervals throughout the test. Any one run gives a wide range of values of $\dfrac{aL}{U_o^2}$. From steady flow data, values of K_s versus Reynolds number were computed. These were used to relate the successive instantaneous conditions of unsteady flow to steady state conditions for the same Reynolds number. With computed values of the inertial coefficient c_1 the combined boundary resistance and momentum flux during unsteady flow was evaluated using Eq. (21).

As previously mentioned, the inertial coefficients c_1 were calculated for the orifices by numerical integration of Eq. (22) from a flow net of the jet profile. This profile is known only approximately and in addition is assumed to be essentially the same over the range of velocity and acceleration of the tests. Therefore, values of K_u can be determined only within some range. Table III gives the computed magnitudes of c_1 together with extreme limits of possible deviations.

Table III

Inertia Coefficients for Unsteady Flow through Orifices

Orifice area ratio	c_1 Based on 4 dia. jet diffusion length	c_1 Possible range of variation	c_1 Assumed for calculation purposes
0.7	1.14	1.00 to 1.50	1.15
0.5	1.27	1.00 to 1.80	1.30
0.3	1.51	1.00 to 2.00	1.50

RESULTS AND CONCLUSIONS

Steady Flow

The experimentally determined steady flow resistance coefficients K_s are presented in Table IV. The coefficients for orifices are in fair agreement with values calculated from the sudden expansion formula. Some dependence on Reynolds number is indicated for the 0.7 area ratio unit. Otherwise the coefficients are essentially constant over the velocity range covered by the experiments. The pipe friction coefficients are given by the relation

$$\frac{1}{\sqrt{f_s}} = 2.0 \log_{10} (\mathbb{R} \sqrt{f_s}) - 0.8$$

where $\mathbb{R}$ = Conduit Reynolds number = $\dfrac{U_o D}{\nu}$

f_s = Steady state pipe friction factor

Substituting $K_s = f_s \frac{L}{D}$ with $\frac{L}{D} = 12$ gives the equation in Table IV for a foot length of test conduit.

Table IV

Steady State Discharge Coefficients

	Area ratio	Loss coef., K_s	Remarks
Orifices	0.7	0.93 0.98	Low Velocities High Velocities
	0.5	3.81	
	0.3	17.00	
Smooth Conduit	1.0	$1/\sqrt{K_s} = 0.59 \log_{10} (\mathbb{R}\sqrt{K_s}) - 0.54$	

Unsteady Flow

The comparison of the unsteady and steady behaviors are given in Figures 4-7 in the form of diagrams of $\frac{K_u}{K_s}$, versus $\frac{aL}{K_s U_o^2}$. Each point plotted on these diagrams was evaluated using K_s from Table IV and the inertial coefficient from Table III.

First it is noted that the plotted points are spread over a considerable area in each diagram. This is due in part to the fact that this form of representation is sensitive to small differences. Therefore, errors are exaggerated. In addition, s the data included a range of velocities, accelerations and rates of change of acceleration (or decelerations) the plotted spread is an indication that the actual unsteady velocity and turbulence distribution and resulting boundary shear and boundary pressures are in some way dependent on these factors.

Nevertheless, it is seen that in each diagram the data falls essentially in two opposite quadrants, indicating definite, even though qualitative, trends in the relative magnitudes of K_u and K_s. Merely to emphasize these trends the data is represented by single straight lines with positive or negative slopes. These slopes are measures of c_2 in Eq. (21) and values of c_2 are indicated. However, it is emphasized that only the sign of the slope, and of c_2, is significant, not the magnitude. In drawing these lines, emphasis was given to the "established phase" portion of the test run, where the rate of change of acceleration is not large.

For accelerated flow through the three orifices, the unsteady coefficient K_u is less than the steady K_s at the same instantaneous velocity. Assuming as previously mentioned that the net flux of momentum is zero for the volume between the measuring stations, the indication is that the boundary resistance during acceleration is less than for the equivalent steady motion. For decelerated flows through these orifices, $K_u > K_s$ and the boundary resistance exceeds that for steady flow.

It is recognized that the results are qualitative, and, because of the uncertainty in the value of the calculated inertial coefficient, this would be the case even in the absence of the factors which were just mentioned as contributing to the spread of observed data.

As previously described, the values of c_1 used to obtain c_2 and K_u were calculated by numerical integration of Eq. (22) from a flow net of the jet profile. This profile is known only approximately and in addition is assumed to be essentially the same over the range of velocities and accelerations of the tests. On the other hand, it should be emphasized that the errors probable or possible in the experimental measurements, or in determining the inertial head drop term, would not alter the stated conclusions.

In the case of the uniform diameter conduit, the magnitude of the boundary resistance during accelerated flow is very nearly the same as for the equivalent steady motion. Nevertheless, in Figure 7 there is a definite indication that K_u/K_s is greater than unity. Thus the case of resistance due to boundary layer shear stresses is affected differently by unsteadiness than resistance associated with the

turbulence generation and diffusion accompanying separation and jet formation. For these data, Schonfeld's theory is used as a guide, and a straight line having a small positive slope is drawn through the plotted points. The relation in Table IV shows K_s to be a function of Reynolds number while the relations derived from Schonfeld's theory (Eqs. 15-17) predicts c_2 and K_u also to be dependent on R. The variation in c_2 is small, however, Using Eqs. (17) and (18) over the range of Reynolds number investigated, c_2 varies only between 0.010 and 0.015. Hence a single straight line with a slope indicating a constant $c_2 = 0.010$ was arbitrarily chosen to qualitatively represent the test data.

For decelerated flow the boundary resistance of the uniform tube is less than for steady flow. In this case, however, there is a clear indication of effects not predicted by Schonfeld's results. As shown, these data can be represented by a family of lines, essentially parallel, one for each deceleration. At any particular velocity, the proportion of boundary resistance to overall potential drop is different, decreasing with increasing deceleration. All of these runs were started from the same steady state velocity, but included different initial impulse periods. From the parallel displacement of the lines for different decelerations, it appears that the flow conditions of the subsequent established phase depend on the previous flow history.

These observations for the uniform tube are consistent with the view that under acceleration the central portion of the stream moves somewhat bodily while the velocity profile steepens, giving higher shear. For deceleration, the reverse seems to hold. In either event, it appears that unsteadiness does not result in marked changes from equivalent steady state flows.

In the case of the orifices, however, it appears that the imposition of a transient results in flows having quite different velocity and turbulence characteristics. This was indicated not only by the relative magnitude of K_u and K_s, but also by what was first thought to be an anomalous experimental result. For decelerated flow through the smaller orifices, it was observed that as the unsteady run proceeded the magnitude of the potential drop changed from less than the equivalent steady state drop (as required to establish the deceleration) to more; i.e., K_a/K_s became greater than 1.0 as the test run proceeded. This observation was repeated on many runs and cannot be attributed to measurement errors. For acceleration through the 0.3 orifice, there was some indication that a corresponding change to $K_a/K_s < 1.0$ occurred late in the run, however, experimental errors could conceivably account for the shift in this case. Such results could only mean that as the unsteady flow proceeded the internal structure of the velocity and turbulence distribution changed to the point that it was no longer comparable to any steady state flow condition.

Such effects as mentioned in the last paragraph clearly indicate that the particular state from which an unsteady run was initiated would affect the subsequent flow history. In fact, more generally it means that any particular unsteady state is dependent on the previous flow history, as seemed to be indicated by the deceleration tests with the uniform tube.

SUMMARY

In summary, it is concluded that the imposition of an unsteady transient produces different effects for the two basic types of flow investigated, as follows:

1. For cases of surface resistance caused by boundary shear stresses

a) With acceleration the resistance is slightly but not appreciably greater than for the equivalent steady state.

b) With deceleration the resistance is appreciably less than for the equivalent steady state.

c) With either acceleration or deceleration, it appears that the internal flow structure is not markedly different from that for steady states.

2. For cases of form type resistance associated with the high shear and generation and diffusion of turbulence accompanying jet formation

a) With acceleration the resistance is appreciably less than for the equivalent steady state.

b) With deceleration the resistance is appreciably more than for the equivalent steady state.

c) For intense jet action as obtained with small orifice to tube diameter ratios, it appears that unsteadiness produces an internal flow structure that is no longer comparable to any steady state condition.

REFERENCES

1. Daily, J. W. and Deemer, K. C., "Measurements of Fluid Friction with Steady and Unsteady Motion," M.I.T. Hydrodynamics Laboratory Report No. 9, July, 1952.

2. Daily, J. W. and Hankey, W. L., Jr.; "Resistance Coefficients for Accelerated Flow through Orifices," M.I.T. Hydrodynamics Laboratory Report No. 10, October, 1953.

3. Olive, R. W., "Resistance Coefficients for Decelerated Flow through Orifices," S.M. Thesis, Course I, M.I.T., 1954.

4. Jordaan, J. M., Jr., "Resistance Coefficients for Unsteady Flow through Fluid Meters," C.E. Thesis, Course I, M.I.T., 1955.

5. Schonfeld, J. C., "Resistance and Inertia of the Flow of Liquids in a Tube or Open Canal," Applied Scientific Research, Vol. A1, 1949.

6. Daily, J. W. and Deemer, K. C., "The Unsteady Flow Water Tunnel at the Massachusetts Institute of Technology," Trans. ASME, Vol. 76, No. 1, 1954, pp. 87-95.

7. Fink, C. H. and Pollis, S. D., "Further Investigation of Fluid Flow through Orifices in Series," B.S. Thesis, Course XIII, M.I.T., 1950.

Velocity and Deceleration, ft. sec. units

a = instantaneous deceleration

U_o = Velocity

17.63 fps

time in seconds

Fig. 8b. Flow characteristics, Deceleration.

Pressure Drop, Percentage of Initial steady state value

83.25 ft.

Velocity and Acceleration, ft. sec. units.

a = instantaneous acceleration

U_o = Velocity

16.62 fps

time in seconds

Fig. 8a. Flow characteristics, Acceleration.

Pressure Drop, Percentage of final steady state value.

73.5 ft.

0 ft.

Orifice Area Ratio = 0.3

Fig. 2. Schematic Section of Tunnel showing Location of orifice.

$$\frac{aL}{K_s U_0^2}$$
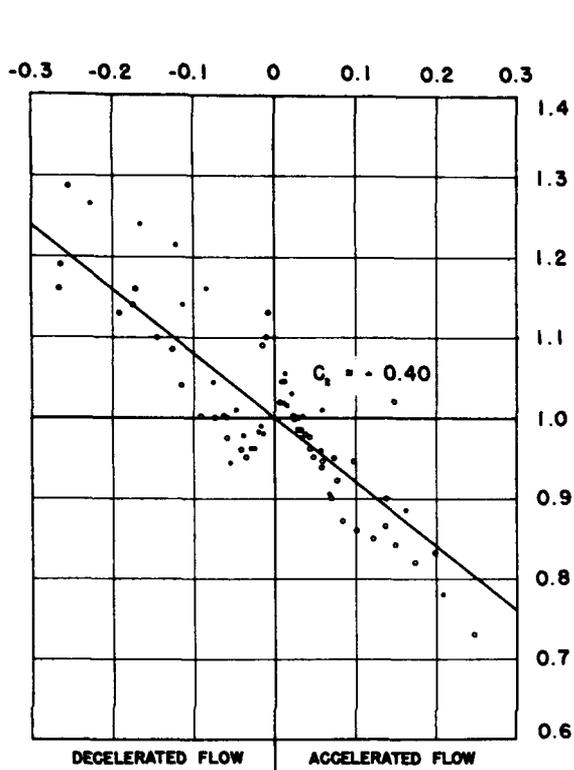
FIGURE 4 ORIFICE AREA RATIO 0.7   FIGURE 5 ORIFICE AREA RATIO 0.5   FIGURE 6 ORIFICE AREA RATIO 0.3
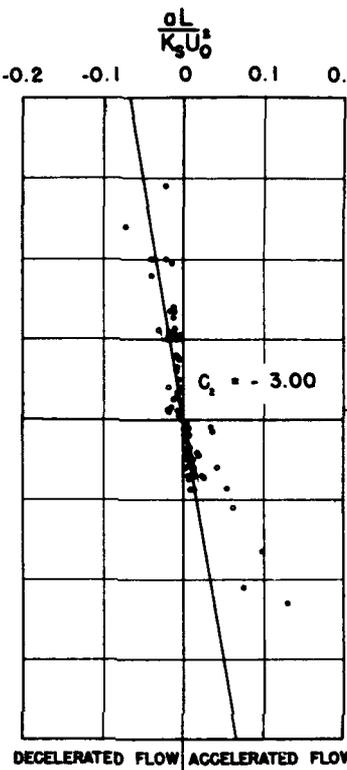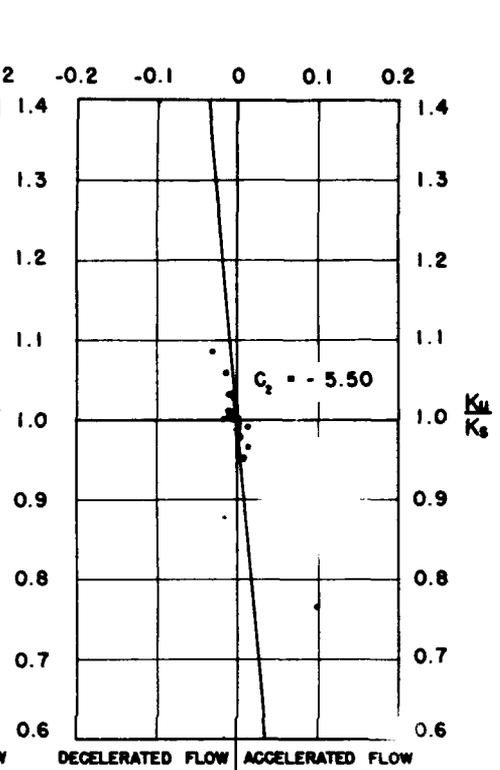
DECELERATED FLOW   ACCELERATED FLOW

$C_2 = -0.40$

$C_2 = -3.00$

$C_2 = -5.50$

$\frac{K_u}{K_s}$
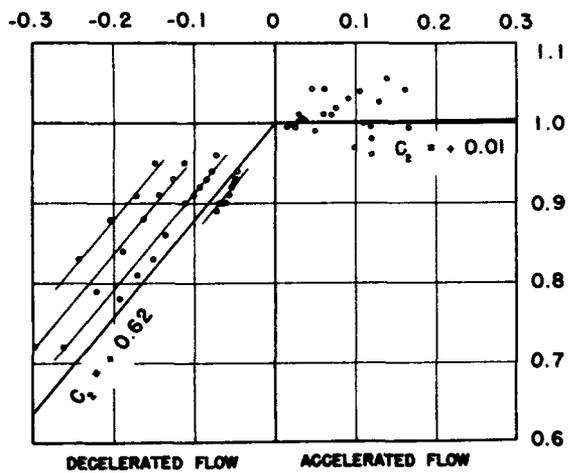
FIGURE 7 SMOOTH CONDUIT (AREA RATIO 1.0)

$C_2 = +0.01$

$\frac{K_u}{K_s}$

0.62

PARAMETRIC   PRESENTATION   OF   UNSTEADY   FLOW

FRICTIONAL   RESISTANCE   COEFFICIENTS

FOR ORIFICES AND SMOOTH CONDUITS